PR3 Studies on Actinides and Fission Products Performed at the KURRI Hot Laboratory

T. Fujii

Graduate School of Engineering, Osaka University

1. Objectives and Allotted Research Subjects

Studies on actinide and fission product nuclides with careful management are being more important for reprocessing, disposal, partitioning, and transmutation processes in the nuclear fuel cycle. Hot laboratory of KURRI is one of core facilities in Japan, in which various nuclides can be handled. This project enhances utilization of the KURRI hot laboratory by opening for fundamental and application studies related to radiochemistry, nuclear chemistry, environmental chemistry, geochemistry, and so on. Allotted research subjects are;

ARS-1 Complexation of actinides with organic substances (T. Sasaki *et al.*).

ARS-2 Solubility of actinide compounds in aqueous media (T. Kobayashi *et al.*).

ARS-3 Leaching of actinides and FPs from fuel debris (N. Sato *et al.*).

ARS-4 Neutron irradiation damage of vitrified waste matrices (T. Nagai *et al.*).

ARS-5 Coordination behavior of actinides in ionic liquds (A. Uehara *et al.*).

ARS-6 Electrochemical behavior of uranium in pyroreprocessing system (Y. Sakamura *et al.*).

ARS-7 Molecular dynamics simulation of actinide and FP ions in melts (N. Ohtori *et al.*).

ARS-8 Fundamental study of fission products for trans-actinide chemistry (Y. Kasamatsu *et al.*).

ARS-9 Isotope fractionation of Sr and Ca by chemical exchange method (R. Hazama *et al.*).

ARS-10 Thermochemical measurement of rare earth complexes (H. Sekimoto *et al.*).

ARS-11 Migration behavior of radiocesium in plants (T. Kubota *et al.*).

ARS-12 Isotopic composition of radionuclides in environmental samples (Y. Shibahara *et al.*).

ARS-13 Behavior of fission products in soil samples (S. Fukutani *et al.*).

ARS-14 Noble gas mass spectrometry of neutron irradiated geological samples (H. Sumino *et al.*).

ARS-15 $^{40}Ar/^{39}Ar$ dating of neutron irradiated minerals and glasses (O. Ishizuka *et al*).

2. Main Results and Contents

ARS-1 and -2 were performed in order to deepen the knowledge of nuclear waste management issues. In ARS-1, for further study on actinides, the formation constants of the Zr-isosaccharinic acid (ISA) complexes were determined by the least squares fitting analysis of the solubility data. Deprotonated Zr-ISA complexes were found at high pH region. In ARS-2, Zr solubility in carbonate solutions was measured and discussed based on the thermodynamic constant and existing activity correction model. The results were compared with Th complexes, and it was found that highly negatively charged Zr carbonate complex was not stable at high ionic strength. ARS-5, 6, 7, and 10 were performed with the viewpoint of pyrochemistry. In ARS-5, the redox reactions of uranium ions in hydrate calcium chloride melts were investigated by electrochemical methods. It was found that the disproportionation of U(V) occurs after the reduction of U(VI) via formation of UO_2, which is not observed in acidic HCl solutions. In ARS-6, the redox mechanism of Se, a fission product element, in molten salts was studied by UV-Vis spectrometry. The results support the electrochemical data, which indicate the complexation of Se with Cu. In ARS-7, the MD simulation for concentrated aqueous LiCl solutions containing La(III) ion. Specific radial distribution functions of O and Cl around La were found. In ARS-10, mutual separation of Nd and Pr in Ca-Li chloride molten salts using molten metallic tin cathode and graphite anode was performed. Reaction mechanisms of Nd and Pr with Sn were clarified. ARS-9 studied isotope fractionation of Ca. A possible fractionation of $^{48}Ca/^{40}Ca$ was found. In ARS-11, Cs-134 and Cs-137 were produced via photonuclear reactions. The isotopic composition of Cs was measured by mass spectrometry and gamma-spectrometry. The effectiveness of this method for correcting the coincidence sum effect was demonstrated. ARS-3, 4, 8, 12, 13, 14, and, 15, focus on environmental chemistry and geochemistry by using KUR, and hence restart of the KUR operation is needed.

3. Summaries of the achievements

New and characteristic chemical, kinetic, structural, and thermodynamic data for actinides and fission products were obtained. These new information encompass aqueous chemistry, pyrochemistry, and isotope chemistry of f-elements and FPs.

PR3-1 Solubility of Tetravalent Metal Hydroxide in the Presence of Isosaccharinic Acid

T. Sasaki, T. Kobayashi, S. Nishikawa, R. Goto, T. Saito[1] and A. Uehara[1]

Graduate School of Engineering, Kyoto University
[1]Research Reactor Institute, Kyoto University

INTRODUCTION: For the safety assessment of radioactive waste disposal, it is very important to predict the solubility limit of M(IV) under relevant conditions. Isosaccharinic acid (ISA), a degradation product of cellulose found in low- and intermediate-level radioactive waste, is known to form strong complexes with radionuclides [1]. Under repository conditions, in the presence of the aforementioned organic acid, the solubility of radionuclides could potentially be enhanced, which could affect the safety assessment of radioactive waste disposal. Since the solubility and complexation behavior of tetravalent actinide (An(IV)) is primarily controlled by the solubility of the sparingly soluble solid phase amorphous hydroxide ($An(OH)_4(am)$) and concentration of complexing agent, respectively, it is necessary to quantify the impact of the complexation ability of the organic acid on the solubility of $An(OH)_4(am)$. Although several reports have investigated the interaction of ISA with tetravalent actinides, the number of reported values of thermodynamic constants such as complex formation constants were considerably limited [1]. In the present study, we focused on the solubility of zirconium in the presence of ISA at a wide range of hydrogen ion concentrations (pH_c). As a tetravalent ion, zirconium is considered to be a chemical analog of tetra-valent actinides (such as Pu(IV)), although different chem-ical characteristics have also been observed. Zirconium is a relevant element in the safety assessment of radioactive waste disposal since it has a high yield in uranium fission products and Zr metal is used as a fuel cladding material in light-water reactors. However, no thermodynamic data on Zr-ISA are available. The formation constants of the Zr-ISA complexes were determined by the least squares fit-ting analysis of the solubility data.

EXPERIMENTS: Calcium isosaccharinate ($Ca(ISA)_2$) was synthesized from α-lactose and converted to NaISA stock solution. An aliquot of NaISA stock solution and HCl and/or NaOH solutions were added to polypropylene tubes to prepare sample solutions at specific hydrogen ion concentrations (pHc) and ISA concentrations. The ionic strength (I) was fixed at $I = 0.5$ mol/dm^3 (M) NaCl. A portion of freshly precipitated $Zr(OH)_4(am)$ solid phase was then added to the tubes. After aging for several weeks, supernatants were filtered through from 10 kDa to 0.45 μm membranes and Zr concentrations were determined by ICP-MS. The solid phases were investigated by XRD within a range of $2\theta = 10°–60°$.

RESULTS: Zr solubility after 14 weeks in the presence of 10^{-3}–10^{-1} M ISA was measured in a pH_c range of 8–12.5 after ultrafiltration through 10 kDa membranes. A steady state was confirmed to be achieved within 10 weeks. In the presence of ISA with a concentration higher than $10^{-2.5}$ M, Zr solubility was found to be higher in comparison with systems with an absence of ISA, depending on the pH_c and ISA concentration [2]. Zr solubility seemed to be almost independent of pH_c under weakly alkaline pH conditions between pH_c 8 and 10, indicating that four OH^- ions are involved in the Zr-ISA complex, provided that $Zr(OH)_4(am)$ is in the solid phase. Zr solubility increased with a slope of approximately 1 above pH_c 10, suggesting that one additional OH^- was involved in the reaction in this pH region. This may be due to further coordination of one OH^- to the Zr-ISA complex or to deprotonation of the hydroxyl group on the main chain of ISA. The Zr solubility at pH_c 9.3 and 12.1 was shown as a function of the total ISA concentration ($[ISA]_{tot}$). The slope against the total ISA concentration was approximately 2, indicating that two ISA molecules were involved in the formation of a Zr-ISA complex. It was noted that no significant peak except that of NaCl(cr) was observed in the XRD patterns of the solid phase aged in the presence of 10^{-1} M ISA.

$$Zr^{4+} + 4OH^- + 2ISA^- \rightleftharpoons Zr(OH)_4(ISA)_2^{2-} \quad (\beta_{142})$$

$$Zr^{4+} + 5OH^- + 2ISA^- \rightleftharpoons Zr(OH)_4(ISA)(ISA_{-H})^{3-} + H_2O \quad (\beta_{152})$$

Taking the isosaccharinate complex formation reactions, the deprotonation of the carboxylic group of ISA [3], the lactonization of ISA [3], and the hydrolysis reactions of Zr [4] into account, Zr solubility ([Zr]) and the total ISA concentration ($[ISA]_{tot}$) can be described as

$$[Zr] = [Zr^{4+}] + \sum_m [Zr(OH)_m^{4-m}] + \sum_{x,y} [Zr(OH)_x(ISA)_y^{4-x-y}]$$

$$[ISA]_{tot} = [ISL] + [HISA] + [ISA^-] + \sum_{x,y} y[Zr(OH)_x(ISA)_y^{4-x-y}]$$

The solubility data in the neutral to alkaline pH range were analyzed to determine the complex formation constants β_{142} and β_{152}. The parameter values are determined in the least squares fitting analysis. The fixed parameters were corrected by SIT. In the alkaline pH region, one of the hydroxyl groups on the alkyl chain of ISA may be deprotonated to form the $Zr(OH)_4(ISA)(ISA_{-H})^{3-}$ complexes.

REFERENCES:

[1] Hummel W et al. Chemical Thermodynamics of Compounds and Complexes of U, Np, Pu, Am, Tc, Se, Ni and Zr with Selected Organic Ligands. Elsevier, North-Holland, Amsterdam (2005).
[2] Sasaki T et al., Radiochim. Acta, **94**, (2006) 489-494.
[3] Rai D et al., J. Solution Chem., **38**, (2009) 1573-1587.
[4] Sasaki T et al., J. Nucl. Sci. Technol., **45**, (2008) 735-739.

PR3-2 Solubility of $Zr(OH)_4$(am) in the Presence of Carbonate Ion in Dilute to Concentrated $NaNO_3$

T. Kobayashi, S. Nakajima, T. Sasaki, A. Uehara[1]

Graduate School of Engineering, Kyoto University
[1]Research Reactor Institute, Kyoto University

INTRODUCTION: For the safety assessment of radioactive waste disposal, it is necessary to predict radionuclide solubility limits under relevant disposal conditions. Actinide elements such as uranium, neptunium and plutonium in the radioactive waste have long half-life and the solubilities are primarily controlled by sparingly soluble hydroxides of tetravalent actinides ($An(OH)_4$(am)). In spite of the strong hydrolysis reaction, the complex formation of An(IV) with carbonate is one of the most important reactions for the reliable prediction of the An(IV) solubility. Since part of low-level wastes (TRU waste) generated from Japanese nuclear reprocessing process contain considerable amount of nitrate salt, an impact of dilute to concentrated $NaNO_3$ on the complex formation of An(IV) carbonate need to be clarified within the context of co-disposal of TRU waste and high level waste. Although a comprehensive literature review has been performed on the thermodynamic constant of actinide including the An(IV) carbonate [1], the literature data on An(IV) carbonate at high ionic strength is still lacking. In the present study, we focus on the complex formation of Zr(IV) carbonate, which is known as an analogue of An(IV). Zirconium is also a relevant element in the safety assessment of radioactive waste disposal, since it has a high yield among the uranium fission products and zirconium metal is used as a fuel-cladding in light water reactors. However, limited thermodynamic data on Zr carbonate at low to high ionic strength is available [2]. Zr solubility in carbonate solution containing 0.1 to 5.0 mol/dm^3 (M) $NaNO_3$ was measured and discussed based on the thermodynamic constant and existing activity correction model.

EXPERIMENTS: Amorphous zirconium hydroxide solid phase ($Zr(OH)_4$(am)) was pre-precipitated and washed with purified water. The $Zr(OH)_4$(am) was then added into the solutions at certain pH, total carbonate concentration ($[C]_{tot}$), and ionic strength (I). The pH was adjusted in the range of pH_c 7 - 12 by HNO_3/NaOH and the ionic strength was controlled to be 0.1, 0.5, 2.0 and 5.0 mol·dm^{-3} (M) by $NaNO_3$. The $[C]_{tot}$ was adjusted to be 0.015 - 0.1 M by $NaHCO_3$. After given aging time, the supernatant of the sample solution was filtrated though ultrafiltration membranes (10 kDa NMWL) and Zr concentration was determined by ICP-MS.

RESULTS: In the presence of carbonate, the solubility of $Zr(OH)_4$(am) increased, indicating the formation of Zr pH_c at $8 < pH_c < 9$, and, after this point, decreased with carbonate complexes. The solubility was independent of increasing pH_c. The solubility at around pH_c 12 was around 10^{-8} M. At pH_c 8.2, the slope of Zr solubility (log [Zr]) against $[C]_{tot}$ was determined to be about 4, suggesting that four carbonates were mainly involved in the dominant Zr carbonate complexes. The relationship between Zr solubility and $[C]_{tot}$ was similar between pH_c 8.2 to 10.9, while no significant relationship was observed at pH_c 11.7. In the pH_c range of 8–9, the solubility at I = 5.0 was about 1.5 orders of magnitude higher than that at I = 0.1, while in contrast, little difference was found between different ionic strengths at $pH_c > 9$. The slope of Zr solubility against $[C]_{tot}$ at I = 0.1-5.0 was also about 4, suggesting that four carbonate ions were involved. In the case that conditions of high ionic strength and $[C]_{tot}$ less than 0.01 M were employed, the slope showed slightly lower values than those at low ionic strength, which suggested the formation of an alternative or additional Zr carbonate complex.

The equilibrium reactions for the formation of the Zr carbonate complexes $Zr(OH)_x(CO_3)_y^{(4-x-2y)+}$ can be described as:

$$Zr^{4+} + xOH^- + yCO_3^{2-} \rightleftharpoons Zr(OH)_x(CO_3)_y^{4-x-2y}$$

$$\log \beta_{1xy} = [Zr(OH)_x(CO_3)_y^{4-x-2y}] / [Zr^{4+}][OH^-]^x[CO_3^{2-}]^y$$

Under the conditions of the present study, the solubility of $Zr(OH)_4$(am) was described as a sum of the concentrations of hydrolysis species and carbonate complexes. The solubility data were analyzed by assuming $Zr(CO_3)_4^{4-}$, $Zr(CO_3)_5^{6-}$, and $Zr(OH)_2(CO_3)_2^{2-}$ from literatures [2]. The β^o_{1xy} and ion interaction coefficient values for $Zr(OH)_x(CO_3)_y^{(4-x-2y)+}$ were determined.

The large ion interaction coefficient values for $Zr(CO_3)_4^{4-}$ and $Zr(CO_3)_5^{6-}$ were a consequence of the minor effects of ionic strength on solubility under high carbonate concentration. The results observed in this study indicated that a highly negatively charged Zr carbonate complex was less stable at high ionic strength, compared to the analogous Th complex [3].

REFERENCES:

[1] Guillaumont R. et al., *Update on the Chemical Thermodynamics of Uranium, Neptunium, Plutonium, Americium and Technetium*. Elsevier, Amsterdam (2003).
[2] Brown P. et al., *Chemical Thermodynamics of Zirconium*. Elsevier, Amsterdam (2005).
[3] Altmaier M. et al., Radiochim. Acta 94, 495-500 (2006).

PR3-3 Electrochemical Analysis for the Redox Reaction of UO_2^{2+} in Calcium Chloride Hydrate Melts

A. Uehara[1], T. Nagai[2], and T. Fujii[3]

[1] *Research Reactor Institute, Kyoto University*
[2] *Nuclear Fuel Cycle Engineering Lab., Japan Atomic Energy Agency*
[3] *Graduate School of Engineering, Osaka University*

INTRODUCTION:

The calcium chloride hexahydrate, $CaCl_2 \cdot 6H_2O$, and similar hydrate melts are of considerable interest as solvents with properties intermediate between those of aqueous solution and molten salts. Activity coefficients, viscosity and structural analyses indicate that the water molecule in $CaCl_2 \cdot 6H_2O$ melts strongly coordinates to the calcium ion showing that this melt is a liquid with the properties of an ionic melt composed of bulky hydrated calcium cations and chloride anions. Namely, this material has advantages such as inorganic-based melt and low melting point. There are a few studies on the electrochemistry of uranium ions in hydrate melts. Cohen [1] has investigated the formation of UO_2^+ in concentrated $CaCl_2$ and LiCl using bulk electrolysis followed by absorption spectrophotometry. Bansal et al. [2] reported that UO_2^{2+} was reversibly reduced to UO_2^+, which can be further reduced to UO_2 in $Ca(NO_3)_2 \cdot 4H_2O$ melt.

In the present study, redox reactions of uranium ions such as U^{4+} and UO_2^{2+} in $CaCl_2 \cdot nH_2O$ hydrate melt (n = 6 – 10) were investigated by electrochemical methods. The chemical behavior of uranium ions in the hydrate melt was compared with that in the other solvents such as high temperature [3] or room temperature [4] molten salts, organic solvents [5] and relatively low concentration solution of hydrochloric acid [6].

EXPERIMENTAL:

For the electrochemical measurements, a three-electrode system was used. A pyro-graphite carbon (Toyo Tanso Co. Ltd.) of 3 mm diameter was used as a working electrode, and the silver|silver chloride (Ag|AgCl) electrode was used as a reference electrode. This reference electrode, in which was put an aqueous solution containing 1 M LiCl along with a Ag wire of 1 mm diameter coated by AgCl. For voltammetric operation, the platinum mesh electrode was employed as a counter electrode. Electrochemical measurement systems, Hz-5000 (Hokuto Denko Co.) were used for the cyclic voltammetry and the linear sweep voltammetry. Controlled-potential electrolysis was carried out in order to identify the electrode reaction. In this experiment, a rotating carbon electrode was employed as a working electrode to enhance the efficiency of the electrolysis. The counter electrode was also a platinum mesh electrode, and the counter phase was separated by glass membrane filter from the objective phase to avoid cyclic redox reaction. After the electrolysis, absorption spectra were measured. A self-registering spectrophotometer UV-1000 (Shimadzu Co.) was used for the measurements over the wavelength from 400 to 900 nm. These measurements were carried out at 300 ± 2 K.

RESULTS:

Voltammograms for the redox reaction of 0.05 M UO_2Cl_2 in 6.9 M $CaCl_2$ were measured by using a platinum working electrode. When the potential scanning rate, v, was from 0.01 to 0.5 V s^{-1}, a cathodic peak current ($I_{c,1}$) was observed at −0.090 V (vs. Ag|AgCl) corresponding to the reduction of UO_2^{2+} to UO_2^+ as Eq. (1);

$$UO_2^{2+} + e^- \rightleftarrows UO_2^+ \quad (1)$$

The $I_{c,1}$ was proportional to the square of v between 0.01 and 0.5 V s^{-1} and the concentration of UO_2^{2+} between 5×10^{-3} and 0.06 M. These results indicated that the $I_{c,1}$ were controlled by the diffusion of UO_2^{2+}. An anodic peak current ($I_{a,1}$) was observed at 0.025 V under the potential sweep rate, v, from 0.1 to 0.5 V s^{-1}. Mid-point potential between cathodic and anodic peaks was found to be −0.058 V. Assuming that the electrode reaction of the $UO_2^{2+}|UO_2^+$ couple is reversible, the diffusion coefficient of UO_2^{2+} at 298 K can be calculated to be 1.7×10^{-7} cm^2 s^{-1}, which was more 10 times smaller than that in diluted electrolyte solutions such as 0.1 M $HClO_4$ (7.3×10^{-6} cm^2 s^{-1}). On the other hand, at $v < 0.1$ V s^{-1}, anodic peak potential shifted positive from 0.025 to 0.165 V. This shift suggests that disproportionation of UO_2^+ occurs after the reduction of UO_2^{2+} as following reaction [2] which is not observed in acidic HCl but room and high temperature ionic liquids [3,4];

$$2\,UO_2^+ \rightleftarrows UO_2^{2+} + UO_2 \quad (2)$$

REFERENCES:

[1] D. Cohen, *J. Inorg. Nucl. Chem.* 32 (1970) 3525.
[2] N.P. Bansal and J.A. Plambeck, *Electrochim. Acta,* 23 (1978) 1053.
[3] T. Nagai, A. Uehara, T. Fujii, O. Shirai, N. Sato and H. Yamana, *J. Nucl. Sci. Technol.* 42 (2005) 1025.
[4] P. Giridhar, K.A. Venkatesan, T.G. Srinivasan and P.R. Vasudeva Rao, *Electrochim. Acta,* 52 (2007) 3006.
[5] L. Martinot, D. Laeckmann, L. Lopes, T. Materne and V. Muller, *J. Alloys Comp.* 185 (1992) 151.
[6] W.E. Harris and I.M. Kolthoff, *J. Am. Chem. Soc.* 69 (1947) 446.

PR3-4 Electronic Absorption Spectra of Selenium in LiCl-KCl Eutectic Melt

Y. Sakamura[1], T. Murakami[1], K. Uozumi[1], A. Uehara[2] and T. Fujii[3]

[1]*Central Research Institute of Electric Power Industry*
[2]*Research Reactor Institute, Kyoto University*
[3]*Graduate School of Engineering, Osaka University*

INTRODUCTION: The electrolytic reduction technique in LiCl-Li_2O melts has been developed for pyrochemical reprocessing of spent oxide fuels [1]. At the cathode, actinide oxides are reduced to their metals:

$$MO_2 + 4\,e^- \rightarrow M + 2\,O^{2-} \qquad (1)$$

where M denotes actinides such as U and Pu. Similar to oxygen, chalcogen fission products such as Se and Te are dissolved into the melt in the form of divalent anion.

Recently, the authors have been studied electrochemical behavior of Na_2Se in LiCl-KCl eutectic melt to extract Se from molten salts [2]. The cyclic voltammograms of glassy carbon electrode indicated that the deposition of Se proceeded in two steps at the anode: the oxidation of Se^{2-} to Se_2^{2-} occurred followed by the oxidation of Se_2^{2-} to Se, which was similar to the electrochemical behavior of sulfur [3]. When Cu was used as the anode, Cu_2Se was deposited at the potentials more negative than the potential of Se deposition. To verify the redox mechanism of Se, a spectroscopic study was conducted.

EXPERIMENTS: LiCl-KCl-Na_2Se mixture was prepared by heating a quartz tube containing LiCl-KCl eutectic (59:41 mole ratio, Aldrich-APL) and Na_2Se (99.8% purity, Alfa Aesar) at 723 K. The Se concentration was determined to be 0.123 wt% by ICP-AES analysis.

LiCl-KCl eutectic (3.075 g) was loaded in a rectangular cylinder quartz cell (10 x 10 mm) used for absorption spectrometry and heated to 723 K in an electric furnace. The experimental apparatus was previously described in detail by Nagai *et al.* [4] The following steps were carried out and then the absorption spectrum of the melt was measured by using an UV/Vis/NIR spectrophotometer (V-570, JASCO).

(1) 0.278 g of the LiCl-KCl-Na_2Se mixture was added.
(2) 0.235 g of the LiCl-KCl-Na_2Se mixture was added.
(3) 0.252 g of the LiCl-KCl-Na_2Se mixture was added.
(4) 0.015 g of Se on a mullite tube was immersed in the melt.
(5) The Se was removed from the melt.
(6) A Cu rod (ϕ2 mm) was immersed in the melt.

RESULTS: Fig. 1 shows absorption spectra of the LiCl-KCl-Na_2Se melt measured during the steps (1)-(6). The absorption peak at 406 nm corresponding to Se^{2-} ions was increased by adding the LiCl-KCl-Na_2Se mixture (steps (1)-(3)). The Se concentration in the melt was 0.022 wt% after step (3). After Se was added into the melt by step (4), an absorption band in the range lower than 406 nm seemed to overlap, which might be due to the formation of Se_2^{2-} ions.

$$Se + Se^{2-} \rightarrow Se_2^{2-} \qquad (2)$$

In fact, the Se concentration in the melt was increased to 0.027 wt% after 1.5 h and the melt became darker brown as visually observed in Fig. 2.

After the Cu rod immersion (step (6)), the absorption peak gradually decreased and went back to 406 nm, which might be due to the decomposition of Se_2^{2-} to give Se^{2-} and Cu_2Se.

$$Se_2^{2-} + 2\,Cu \rightarrow Se_2^{2-} + Cu_2Se \qquad (3)$$

In summary, the results of this spectroscopic study are consistent with the results of electrochemical measurement [2]. However, the Se concentration was finally decreased to 0.013 wt% and the absorption peak at 406 nm became low. The reasons for mass loss should be clarified.

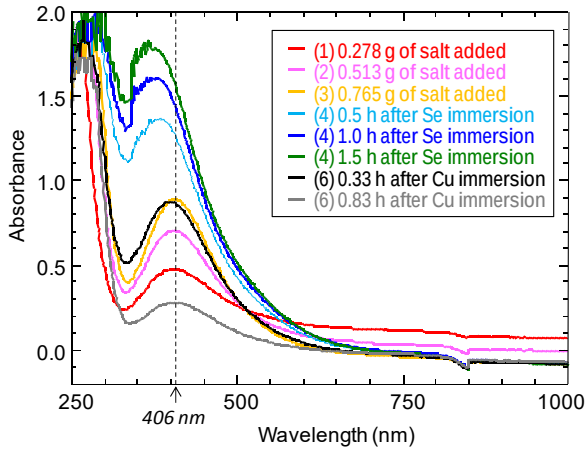

Fig. 1 Absorption spectra of LiCl-KCl-Na_2Se melt measured during steps (1)-(6).

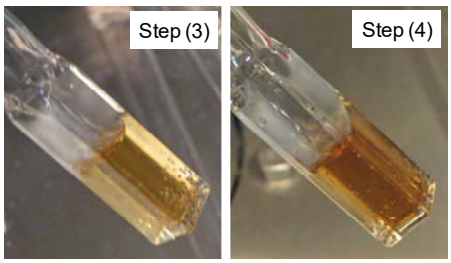

Fig. 2 The quartz cell containing LiCl-KCl-Na_2Se melt after steps (3) and (4).

REFERENCES:

[1] Y. Sakamura and M. Akagi, Nucl. Technol. **179** (2012) 220-233.
[2] Y. Sakamura and M. Iizuka, Proc. The 48th Symposium on Molten Salt Chemistry, p. 1-2, Niigata Univ., Japan, Nov. 24-25, 2016, in Japanese.
[3] D. Warin, Z. Tomczuk and D.R. Vissers, J. Electrochem. Soc., **130** (1983) 64-70.
[4] T. Nagai, T. Fujii, O. Shirai and H. Yamana, J. Nucl. Sci. Technol., **41** (2004) 690-695.

PR3-5 Coordination Structure around La^{3+} Ion in Concentrated Aqueous Solutions of LiCl

N. Ohtori, Y. Ishii[1], A. Uehara[2] and T. Fujii[3]

Department of Chemistry, Niigata University

[1]Graduate School of Science and Technology, Niigata University

[2]Research Reactor Institute, Kyoto University

[3]Department of Sustainable Energy and Environmental Engineering, Graduate School of Engineering, Osaka University

INTRODUCTION: Recently, hydrate melts such as concentrated alkali halide aqueous solutions attract some attention as one of the novel candidates for solvents useful for reprocessing of spent nuclear fuels[1]. We performed molecular dynamics (MD) simulation of LiCl aqueous solutions containing uranyl ion and reported some results such as diffusion coefficients and average local structure around uranyl ion in the previous report[2]. Then, we analyzed coordination structure around uranyl ions in 14 M LiCl aqueous solution in more detail and compared the results with experimental results[3]. In this study, we report the results of MD simulation for concentrated aqueous solutions of LiCl containing La^{3+} ion and discuss coordination structure around La^{3+} ion.

CALCULATION: MD calculation has been performed under *NVE* ensemble. The SPC/E model was used for water molecule. The other parameters were taken from the references cited in [3, 4]. The water molecules were constrained by SHAKE algorithm. The number of particles included in the simulation cell is shown in Table 1. Time step was 1.0 fs.

RESULTS: Figures 1 and 2 show the radial distribution function and coordination number of O atom or Cl^- ion around La^{3+} ion in 14 M aqueous solution of LiCl. Although, regarding distances between La^{3+} and O or Cl^-, the present MD results are in good agreement with those of first-principles MD[5], regarding the peak heights, it shows poor agreements. Although the experimental results of coordination number follow rather simple composition ratio, the present MD results show some underestimates in La-Cl and overestimates in La-O.

Table 1 Number of particles included the simulation cell for aqueous solutions of LiCl containing La^{3+} ion.

$[Cl^-]$ / mol dm^{-3}	Number of unit			
	H_2O	Li^+	Cl^-	La^{3+}
0	1108	0	3	1
1	1086	20	23	1
3	1040	60	63	1
8	924	160	163	1
14	782	280	283	1

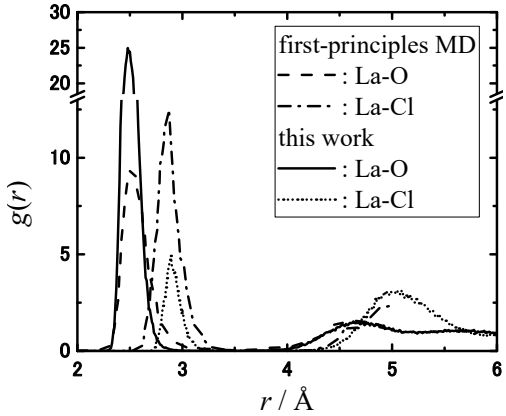

Fig.1 Radial distribution function of O atom or Cl^- ion around La^{3+} ion in 14 M aqueous solution of LiCl.

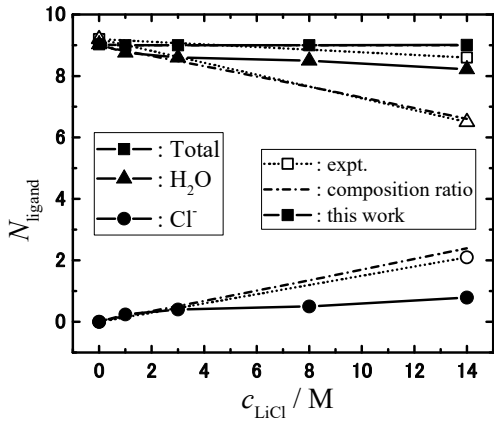

Fig. 2 Concentration dependence of coordination number of O atom or Cl^- ion around La^{3+} ion in aqueous solution of LiCl.

REFERENCES:

[1] A. Uehara, O. Shirai, T. Fujii, T. Nagai and H. Yamana, *J. Appl. Electrochem.*, **42**, 455(2012).

[2] N. Ohtori, Y. Ishii, Y. Nagata, A. Uehara, T. Fujii, H. Yamana, K. Minato and Y. Okamoto, KURRI Progress Report 2012, PR2-1(2013).

[3] N. Ohtori, Y. Ishii, A. Uehara, T. Fujii, H. Yamana, and Y. Okamoto, KURRI Progress Report 2013, PR1-12(2014).

[4] S. Díaz-Moreno, S. Ramos, and D.T. Bowron, *J. Phys. Chem. A*, **115**, 6575 (2011).

[5] L. Petit, R. Vuilleumier, P. Maldivi, and C. Adamo, *J. Phys. Chem. B*, **112**, 10603 (2008).

28P3-7

PR3-6 Study of Isotope Separation of Strontium and Calcium via Chemical Exchange Reaction

R. Hazama, Y. Sakuma[1], T. Yoshimoto, T. Fujii[2], T. Fukutani[3] and Y. Shibahara[3]

Graduate School of Human Environment, Osaka Sangyo University

[1]Research Laboratory for Nuclear Reactors, Tokyo Institute of Technology,

[2]Graduate School of Engineering, Osaka University
[3]Research Reactor Institute, Kyoto University

INTRODUCTION: Calcium is congener of strontium and easy to handle to check the isotope effects. By utilizing chemical separation method for calcium isotope effect in liquid-liquid extraction (LLE), an appropriate crown-ether can be used not only for separation of metal ions, but also for separation of isotope[1].

EXPERIMENTS: Isotopic enrichment occurs according to the following chemical exchange reaction:

$$^{40}Ca^{2+}_{(aq)} + {}^{48}CaL^{2+}_{(org)} \rightarrow {}^{48}Ca^{2+}_{(aq)} + {}^{40}CaL^{2+}_{(org)} \quad (1)$$

where L represents macrocyclic polyether(18-crown-6). A 20 ml aqueous solution (3M $CaCl_2$) and 200 ml organic solution (0.07M DC18C6 in chloroform) were stirred by a magnetic stirrer for 30 m/60 m at room temperature and separated. This LLE was iterated six times (1－6)[2].

Natural samples of Ca must be purified to remove potassium because ^{40}K interferes on ^{40}Ca, thus purification by cation exchange resin (DOWEX 50WX8) was conducted prior to isotope analysis. Samples with ultrapure 0.1M HNO_3 were loaded onto this ion exchange column in order to extract the Ca-fraction. After rinsing the column with ultrapure 8M HNO_3 the Ca-fraction was collected, evaporated to dryness and then dissolved in ultrapure HNO_3 to form $Ca(NO_3)_2$. About 30 μg of Ca in the nitrate form (1 μL) are loaded onto the single Re filament in combination with the so called "sandwich-technique" of Ta_2O_5-activator, which stabilizes the signal intensity [3].

All Ca isotope measurements were carried out by the TIMS, KURRI. The TRITON multicollector is operated in positive mode with a 10 kV acceleration voltage and equipped with nine Faraday cups as detection system, but cannot account for the dispersion of the whole Ca isotope mass range from 40 to 48 amu. During the first sequence, the masses of 40, 42, 43 and 44 are measured simultane-ously and during the second sequence, the masses 43, 44 and 48 are measured. Table 1 shows a summary of the experimental conditions for Ca isotope analysis using TIMS.

Property	Setting
Accelerating voltage	10 kV
Source vacuum	1 × 10^{-7} mbar
Analyzer vacuum	6 × 10^{-9} mbar
Faraday cup	9
Baseline(each block)	Delay time: 10 s Integration time: 16 s
Data collection	Blocks/run: 6 Scans/block: 10 Integration time: 4 s Idle time: 3 s
Analyzing temperature	1500 – 1580 ℃: 3A Boiling point@1 atm: 1487℃

Table 1. Experimental condition used for Ca isotope analysis by TIMS.

RESULTS: The linearity of the plots in Fig. 1 indicates that the isotope effects show the normal mass dependence.

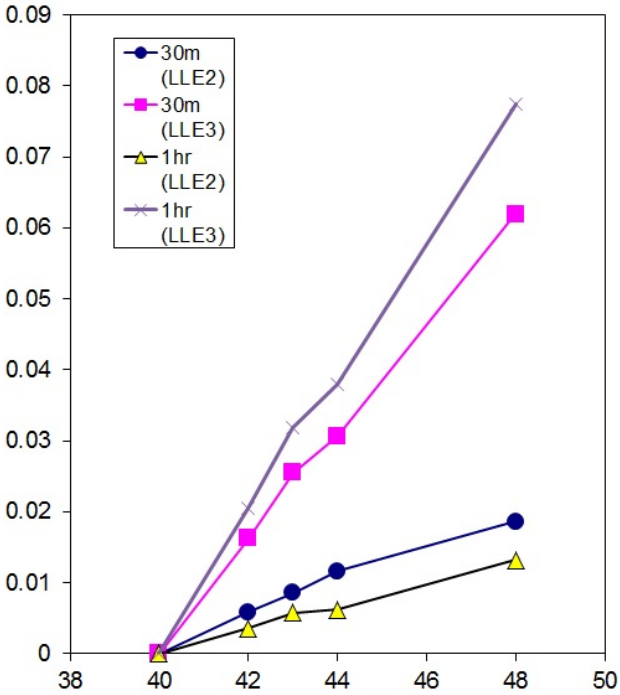

Fig. 1. Mass dependence of observed Ca isotope separation: Preliminary. Circle/Square:30m , Triangle/Cross: 60m for stirring and standing for separation, respectively.

REFERENCES:

[1]B.E. Jepson *et al*., J. Inorg. Nucl. Chem.**38**(1976)1175.
[2]R. Hazama *et al*., Proc. 6th Recontres du Vietnam, The Gioi Publishers (2007) 383: arXiv: 0710.3840.
[3]A. Heuser *et al*., Int.J.Mass Spec. **220**(2002)385.

28P3-9

PR3-7 Mutual Separation of Nd and Pr by Molten Salt Electrolysis

H. Sekimoto[1], A. Uehara[2], T. Fujii[3]

[1]*Department of Physical Science and Materials Engineering, Iwate University*
[2]*Research Reactor Institute, Kyoto University*
[3]*Department of Sustainable Energy and Environmental Engineering, Osaka University*

INTRODUCTION:

Mutual separation of Nd, Dy and Pr is essentially important for the recycling of the neodymium magnet. Uehara et al. reported on the mutual separation of La and Nd utilizing the disproportionation reaction of Nd(II) to metallic Nd and Nd(III) in LiCl-KCl molten salt [1]. This technique seems quite attractive comparing with the conventional processes such as the ion exchange process and the solvent extraction process in terms of the environmental load. We have investigated the absorption spectra of ions of Nd, Dy and Pr in $CaCl_2$-LiCl eutectic molten salt and the electrochemical behaviors them [2,3]. In this study, the mutual separation of Nd and Pr in $CaCl_2$-LiCl eutectic molten salt using molten metallic tin cathode and graphite anode was examined.

EXPERIMENTS:

Electrochemical experiments and the absorption spectrometry were conducted in the argon atmosphere, where the concentration of oxygen and water was controlled below 1 ppm. 4 g of metallic tin, 6.20 g of $CaCl_2$, and 3.80 gram of LiCl were weighed and inserted in a quartz optical cell attached with cylindrical quartz tube. The sample heated at 750 °C in an electric furnace to be melt. 0.0370 g of $NdCl_3$ and 0.0384 g of $PrCl_3$ were dissolved in the molten salt, and thus, the initial concentration of Nd(III) and Pr(III) in the molten salt was 0.211 mass% and 0.217 mass%, respectively. The temperature was then controlled to be kept at 700 °C. After that, a tungsten rod was immersed in the molten metallic tin phase to make working electrode. A graphite rode and the Ag-AgCl reference electrode also immersed in the molten salt phase as counter electrode and reference electrode respectively. Potentiostatic electrolysis was conducted at -1300 mV vs the Ag-AgCl electrode for 2700 s.

Absorbances of Nd(III) and Pr(III) dissolved in the $CaCl_2$-LiCl eutectic molten salt were measured before and after electrolysis. The concentrations of neodymium and praseodymium in the molten salt phase and metallic tin phase were determined by ICP-OES.

RESULTS:

Figure 1 shows absorption spectra of the molten salt containing Nd(III) and Pr(III). Solid line and dotted line corresponds the spectrum before and after electrolysis, respectively. The peak intensity at 589 nm which is due to the absorption by Nd(III) decreased from 0.62 to 0.34. The peak intensity at 1546 nm which is due to the absorption by Pr(III) decreased from 0.082 to 0.060. This means that Nd(III) and Pr(III) were electrochemically reduced. The concentration of Nd and Pr in the molten salt after the electrolysis determined by ICP-AES were 0.145 mass% and 0.148 mass% and, respectively. The concentration ratio of Nd and Pr in the molten salt after the electrolysis was 0.98, which was almost same value as that before the electrolysis; 0.97. On the other hand, the concentration of Nd and Pr was 0.0566 mass% and 0.0702 mass%, respectively. The concentration ratio of Nd and Pr in the molten salt after the electrolysis was 0.81. In $CaCl_2$-LiCl eutectic molten salt, Nd(III) is reduced to Nd(II) which is then decomposed to metallic neodymium and Nd(III) with disproportionation reaction, while Pr(III) is reduced to Pr [3]. It is considered that Pr(III) was reduced on molten metallic tin cathode to form Sn-Pr alloy. But, Nd(III) is reduced to on the tin cathode Nd(II), which decomposed to metallic neodymium and Nd(II) in molten salt phase. A part of the metallic neodymium react with Sn to form Sn-Nd alloy. Consequently, the concentration ratio of Nd and Pr in metallic tin decreased comparing that in molten salt.

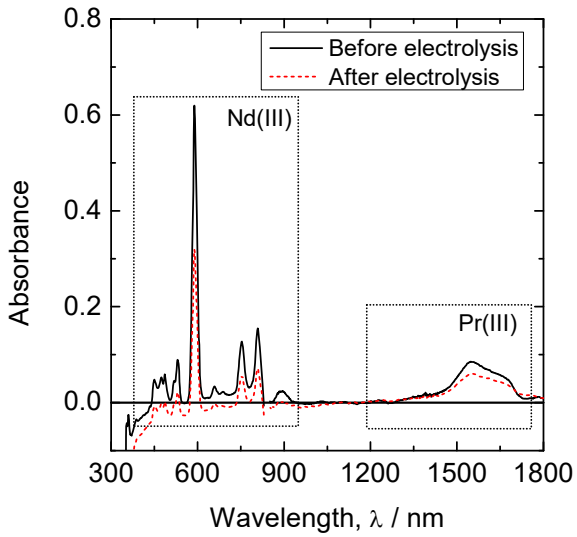

Fig. 1. Absorption spectra of the molten salt containing Nd(III) and Pr(III). Solid line and dotted line corresponds the spectrum before and after electrolysis, respectively.

REFERENCES:

[1] A. Uehara, K. Fukasawa, T. Nagai, T. Fujii, and H. Yamana, *J. Nuclear Mater.*, **414**, 336 (2011).
[2] H. Sekimoto, A. Uehara, T. Fujii, H. Yamana, KURRI Progress report, (2014).
[3] H. Sekimoto, A. Uehara, T. Fujii, H. Yamana, KURRI Progress report, (2016).

PR3-8

Correction of Coincidence Sum Effect by Using ^{134}Cs and ^{137}Cs Produced through a Photo Nuclear Reaction

T. Kubota, S. Fukutani, Y. Shibahara, T. Ohta[1]

Research Reactor Institute, Kyoto University
[1]Central Research Institute of Electric Power Industry

INTRODUCTION: The migration of radioactive cesium in plants is often investigated with respect to the competition of potassium. Among potassium isotopes, ^{43}K is useful for tracer experiments. This nuclide can be produced from calcium and is referred to carrier free; its radioactivity can be regulated to enough for experiments. The immediate purification of ^{43}K is required because of its short half life, $T_{1/2}$ = 22.3 h. In this study the purification methods are investigated by using ^{134}Cs and ^{137}Cs, instead of ^{43}K, for the convenience of experiment and on considering that both elements are alkaline metals and hence exhibit a similar chemical behavior. In addition, these cesium nuclides were used to correct coincidence sum effect on γ-spectrometry. Without attention to this effect, the evaluation of ^{134}Cs radioactivity would be incorrect. In order to correct the coincidence sum effect, ^{134}Cs and ^{137}Cs were produced through a photo nuclear reaction and the isotopic ratios of ^{134}Cs to ^{137}Cs measured by Thermal Ionization Mass Spectrometry (TIMS) and γ-spectrometry were compared.

EXPERIMENTS: Radioactive cesium nuclides, ^{134}Cs and ^{137}Cs, were produced through irradiation of barium chloride with photons generated by the bombardment of platinum with high-energy electrons. The barium target material was encapsulated in a quartz tube under vacuum. The irradiated material dissolved with H_2O was added with ammonium carbonate [1] or ammonium oxalate [2] to precipitate barium and thus to purify cesium in the solution. The cesium solution, containing ammonium chloride and/or oxalate, was evaporated to remove these salts. An aliquot of the purified solution was used to determine an isotopic ratio by TIMS [3] and the obtained value was converted to activity ratio of ^{134}Cs/^{137}Cs. A 5 mL of the solution was used to determine radioactivity with a high-purity Ge semiconductor detector where the sample was located 0 cm and 10 cm away from the detector. The radioactivity of ^{134}Cs and ^{137}Cs was evaluated from 605-keV and 661-keV gamma ray, respectively.

RESULTS: The irradiated barium chloride sample was stored for four months prior to cesium separation. The cesium separation was conducted by precipitating barium carbonate or barium oxalate. Both precipitation methods showed high decontamination factor and high cesium recovery. However, ammonium carbonate was adopted to remove barium because the deposition of oxalate occurred and this remaining cannot be removed by evaporation. The activity ratio of ^{134}Cs/^{137}Cs in purified cesium solution was determined by TIMS and g-spectrometry. The isotopic ratio of ^{134}Cs/^{137}Cs measured by TIMS was 0.126, which was equivalent to 1.824 in activity ratio. The radioactivity ratio of ^{134}Cs/^{137}Cs measured by γ-spectrometry was 1.63 and 1.82 at 0 cm and 10 cm from the detector surface, respectively (Fig. 1) and this difference was ascribed to the coincidence sum effect. The value obtained at 10 cm was agreement with the value by TIMS, which means the sum effect can be ignored by keeping a distance of 10 cm from the detector surface.

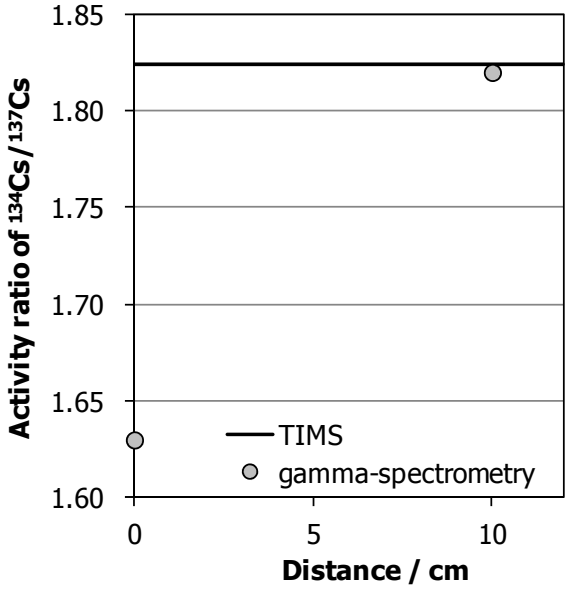

Fig. 1. Activity ratio of ^{134}Cs and ^{137}Cs as a function of distance between the sample and the detector surface.

REFERENCES:

[1] Handley *et al.*, Anal. Chem., **31** (1959) 332.
[2] Sugihara *et al.*, Anal. Chem., **31** (1959) 44.
[3] Y. Shibahara *et al.*, J. Nucl. Sci. and Tech., **54**, (2016) 158-166.